JOURNAL OF AIRCRAFT
Vol. 44, No. 1, January–February 2007

Calibration and Use of Goodrich Model 0871FA Ice Detectors in Icing Wind Tunnels

Richard K. Jeck*
Federal Aviation Administration, Atlantic City, New Jersey 08405

DOI: 10.2514/1.23543

A simple, new, triple-calibration scheme is developed for Goodrich (formerly Rosemount) model 0871FA ice detectors. The analog output voltage is equated not only to the usual liquid water concentration, but to accurately computed ice mass-and-depth accretion rates on the sensitive element of the detector. The three different calibration constants vary from detector to detector, but are related through invariant equations that are probe-independent. Thus, the relations can serve as universal calibration equations for *any* 0871FA detector. The method is demonstrated for three detectors in the steady-state conditions of an icing wind tunnel. Other observed characteristics of 0871FAs are described to help users understand the behavior of these detectors during operation. Close-up video confirms that irregularities that sometimes appear in the analog output signals are due to incomplete shedding of the ice during the heating cycles under certain conditions. The tunnel experiments also suggest that a combination of 0871FA and a fast-response liquid water sensor can be useful for real-time tunnel calibration checks, rapid adjustment, and subsequent continuous monitoring and documentation of tunnel *icing* conditions. A traveling pair of these probes can be a new way to set and/or compare intended identical icing conditions from one icing wind tunnel to another.

Nomenclature

C_d	=	0871FA ice depth calibration constant m/V
C_m	=	0871FA ice mass calibration constant, V/g
D	=	depth of ice accreted on the 0871FA sensing tube
E_{tot}	=	total droplet collection efficiency
$f(n)$	=	a function of the freezing fraction n
k	=	0871FA water catch calibration constant, V/s per $(\text{m/s} \cdot \text{g/m}^3)$
V	=	analog output signal from 0871FA, V
V_{trip}	=	output voltage that trips the heater
V_0	=	baseline (uniced) output voltage
$\beta_{\max}$	=	the maximum value of the local droplet collection efficiency
ρ	=	density of accreted ice 880 to 917 kg/m^3
ΔD	=	ice depth per cycle, mm
ΔM	=	ice mass per cycle, mg
Δt	=	cycle rise time, s
ΔV	=	output voltage span, $V_{\text{trip}} - V_0$

I. Introduction

THE Goodrich† series 0871 of patented icing detectors‡ was developed in the mid 1960s in response to the need for a reliable ice warning system for aircraft. Currently, various models in this series are used on a variety of civil and military aircraft. The 0871FA model (hereafter called an 0871FA, or simply a *probe*), in particular, has a variable output signal that is proportional to the amount of ice accreted on the sensing element. This makes it a useful tool for icing research or test flights and for icing wind tunnels.

A. Principle of Operation

Figure 1 shows the physical appearance of the device. The sensitive element is the 1-in. (2.54-cm) long, 1/4-in. (6.35-mm) diam cylindrical tube that vibrates imperceptibly at about 40 kHz due to a magnetostrictive driver embedded inside the tube.

As ice builds up on the tube, the vibration is slowed slightly and the device outputs a 1 to 5 V analog signal that is proportional to the reduction in frequency and to the mass of the accumulated ice. When a certain ice mass is reached, nominally about 70 mg, equivalent to a peak thickness of about 0.5 mm on the windward surface of the tube, an internal heater is automatically energized to melt and remove the accumulated ice. This occurs at an output voltage of about 5 V. The output signal then drops to its baseline (uniced) value, the heating stops, and the ice accumulation can resume as soon as the surface temperature of the sensing tube cools to below 0°C. An example of the analog output signal is shown in Fig. 2. The ascending slope during the accumulation intervals is proportional to the ice accretion rate. In the constant icing conditions of an icing wind tunnel (hereafter simply referred to as a *tunnel*), the 0871FA output signal will increase linearly with time during the sensing intervals.

B. Calibration Requirements

For use as a simple ice warning device on an airplane, the exact relationship of accreted mass-to-voltage output is not critical. Each time a nominal amount of ice has accreted, an ice warning light is illuminated in front of the pilot. For research quality measurements, however, the variable output signal needs to be calibrated in terms of accreted ice mass, ice accretion rate, or supercooled water concentration [usually called the liquid water content (LWC)] associated with the cloud or spray droplets in the airstream.

The 0871FAs are not routinely calibrated by the factory before sale, but as long as the analog output voltage span is about 4 V, the probe is expected to nominally accrete about 0.5 mm of ice per cycle. Some practitioners use this nominal amount as a generic (one size fits all) calibration factor, perhaps being unaware that some probes require considerably more or considerably less ice per volt or per cycle. This has been documented by other researchers [1–3] who used these probes as LWC indicators on instrumented airplanes and

Received 28 February 2006; revision received 5 July 2006; accepted for publication 8 July 2006.

*Research Physicist/Meteorologist, Flight Safety Branch (AJP-6350), Airport and Aircraft Safety R&D Division, William J. Hughes Technical Center; richard.jeck@faa.gov.

†Sensor Systems, Goodrich Corporation, 14300 Judicial Road, Burnsville, MN 55306-4898 is incorporated as Rosemount Aerospace, Inc. Ice detectors made by Goodrich are commonly referred to as "Rosemount" ice detectors by the industry.

‡The Federal Aviation Administration does not officially endorse any goods, services, material, or products of manufacturers that may be named in this article.

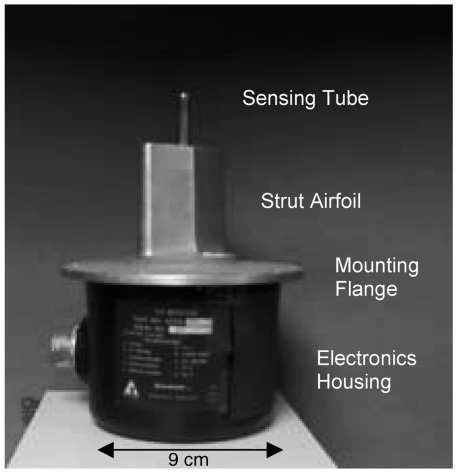

Fig. 1 The model 0871FA ice detector.

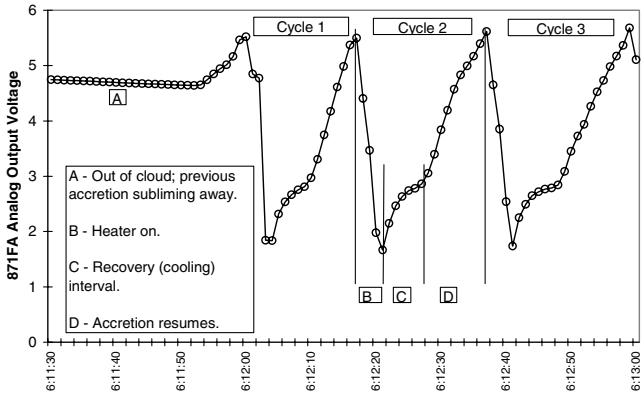

Fig. 2 Actual example of the analog output voltage from an 0871FA ice detector.

who pointed out the need for individual calibration in controlled conditions.

Different 0871FAs can also have voltage rise rates that differ by as much as a factor of five in the *same* icing conditions. These differences are due to a nonobvious interplay between the electronic sensitivity and the actual voltage output span for each probe. The relative effect of the electronic sensitivity and the output voltage span has been a source of confusion and has never been adequately explained before. For research purposes, one needs to know the exact conversion of output volts to ice depth (mm) or rate of accretion (mm/min) for each individual probe. In the present case, three different 0871FAs had been used on icing research flights, and calibration checks were needed in order to convert the output voltages into reliable icing rates.

In addition, some of the older probes still in use sometimes display anomalous or seemingly erratic behavior of the voltage output signal, which has never been completely explained. And, finally, two of the probes tested here had been used in some large droplet (freezing drizzle or freezing rain) icing conditions, and so there was a need to know whether or not the calibration is different for large supercooled drops. For all these reasons, calibration and performance tests were needed in the controlled conditions of an icing wind tunnel where each of these concerns could be investigated. This paper reports on the results of these tests, provides some new insights into the response of these probes, and proposes some new applications of 0871FAs that were suggested by these experiments.

II. Theory

A. Basic Equations

The following variables are of potential interest to users of the icing detector.

Ice-mass-related quantities: 1) mass (mg) deposited per icing cycle, 2) mass deposition rate (mg/s), 3) mass (mg) per volt of output signal, 4) probe sensitivity (V/g), and 5) water concentration, LWC (g/m^3).

Ice-depth-related quantities: 1) depth (mm) of ice deposited per icing cycle, 2) depth rate (mm/s), 3) depth (mm) per volt of output signal, and 4) probe sensitivity (V/mm).

These all require knowing the relationship (calibration) between the quantity of interest and the output voltage from the probe.

The magnitude of the voltage increase, $V - V_0$, is a measure of the mass M or depth D of the accreted ice. Experimentally then, by measuring the voltage rate of increase, $\mathrm{d}V/\mathrm{d}t$, one can obtain the rate of ice accretion, $\mathrm{d}M/\mathrm{d}t$ or $\mathrm{d}D/\mathrm{d}t$.

The basic equations are

$$V - V_0 = C_m M \tag{1}$$

and the mass accumulation (water catch) rate

$$\mathrm{d}M/\mathrm{d}t = (1/C_m)\,\mathrm{d}V/\mathrm{d}t \tag{2}$$

and the icing depth rate

$$\mathrm{d}D/\mathrm{d}t = C_d\,\mathrm{d}V/\mathrm{d}t \tag{3}$$

where C_m and C_d are two different calibration constants (constants of proportionality) relating $\mathrm{d}V/\mathrm{d}t$ to different measures of the ice accretion process. The constant C_m defines the basic sensitivity of the probe: the change in output voltage as a function of accreted ice mass [Eq. (1)] or the rate at which the output voltage changes as a function of the mass rate [Eq. (2)]. The constant C_d is the factor by which the voltage rise rate $\mathrm{d}V/\mathrm{d}t$ must be multiplied in order to give the icing depth rate. We shall see that the calibration constants C_m and C_d can be simply obtained from measured values of $\mathrm{d}V/\mathrm{d}t$ in the steady-state conditions of an icing wind tunnel.

B. Icing Depth Rate

From Eq. (3), the depth of ice deposited per cycle is given by

$$\Delta D = C_d \bullet \Delta V \tag{4}$$

For a given probe, ΔD per cycle is a constant value no matter what the icing conditions, airspeed (typical airplane speeds), or LWC. It depends only on the product of the output voltage span, $\Delta V = V_{\mathrm{trip}} - V_0$, and the sensitivity, C_d in millimeters per volt, of the probe. This is the interdependency that can be confusing to the user. The effect of a reduced voltage span may be intuitive, but the effect of a greater or lesser sensitivity may not be. The larger the value of C_d, the thicker the ice deposit per cycle for a given ΔV. But a larger C_d does not mean a more sensitive probe. Rather, the opposite interpretation applies. A larger C_d means a less-sensitive probe because it takes more ice to produce a volt of output from the probe. Thus, it takes longer to accumulate the number of millimeters needed to raise the output voltage up to V_{trip}. The constant C_d may be thought of as the gain factor needed to boost the probe output $\mathrm{d}V/\mathrm{d}t$ so that it will indicate the true icing rate.

The true icing depth rate at the leading edge of the cylindrical sensing tube is independent of the probe calibration and can be accurately computed from

$$\mathrm{d}D/\mathrm{d}t = \beta_{\max} \bullet \mathrm{TAS} \bullet \mathrm{LWC} \bullet f(n)/\rho \tag{5}$$

where $f(n)$ is a dimensionless and unknown, except $f(1) = 1$ and $f(0) = 0$. (In the tunnel tests, the air temperature was kept sufficiently low to ensure that $n = 1$ for all calibration runs.) Values of β and n were obtained from LEWICE [4], a computerized droplet impingement and ice accretion code produced by the NASA Glenn Research Center and commonly used by aircraft icing engineers in the United States. Figure 3a shows a plot of β along the circumference of a 6.35-mm-diam cylinder, intercepting 15-μm- or 20-μm-diam drops at 62 and 144 m/s (120 and 280 kt). $\beta_{\max}$ is the peak value, which occurs along the lengthwise centerline (stagnation

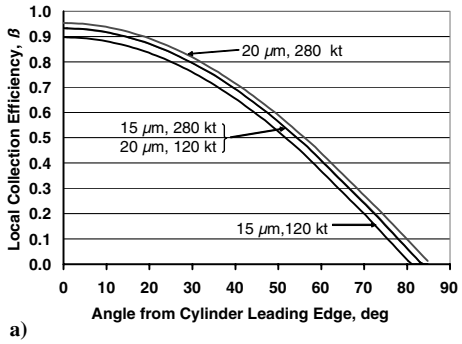

a)

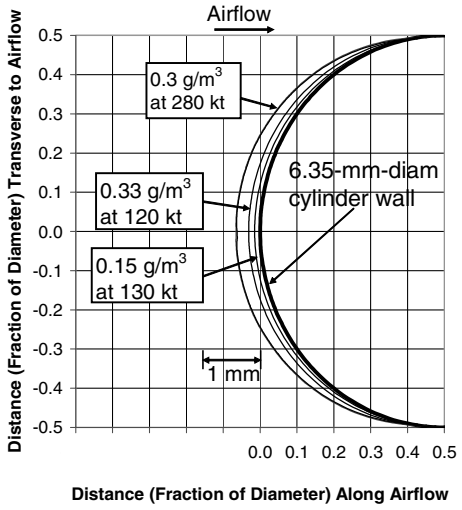

b)

Fig. 3 LEWICE-computed variables for a 6.35-mm-diam cylinder: a) local collection efficiencies and b) ice layers for 10-s exposures to 15-μm- or 20-μm-diam drops.

line) of the uniced or conformally iced cylinder. For the convenience of the interested user, some values of $\beta_{\max}$ are listed in Table 1.

LEWICE also computes $\mathrm{d}D/\mathrm{d}t$ independently of Eq. (5) by modeling the physics (aerodynamics and thermodynamics) of droplet impingement, heat transfer, and ice accretion processes around the circumference of the cylinder. Figure 3b illustrates the ice deposits computed by LEWICE on a 6.35-mm-diam cylinder. Whereas LEWICE computes ice depths around the circumference, Eq. (5) gives results that agree with LEWICE for a single value of $\beta_{\max}$. This gives confidence in the adequacy of Eq. (5) for this much simpler calibration method.

C. Mass Accretion Rate

Similarly, the mass rate, or water catch rate, independent of the probe calibration, can be computed from

$$\mathrm{d}M/\mathrm{d}t = E_{\text{tot}} \bullet \text{TAS} \bullet \text{LWC} \bullet \text{area} \bullet f(n) \tag{6}$$

where area is the cross-sectional area (1.6×10^{-4} m^2) of the 2.54 cm (1 in.) by 0.635 cm (1/4 in.) sensing tube. As another convenient reference, values of E_{tot} computed by LEWICE are listed in Table 1. Equation (6) also gives values of mass rate that agree closely with those obtained from LEWICE.

D. Voltage Rise Rate

Knowing that the voltage rise rate is proportional to the product of the (supercooled) LWC and true airspeed (TAS), another simple relationship between the output voltage and these two variables can be written

$$\mathrm{d}V/\mathrm{d}t = k \bullet \text{TAS} \bullet \text{LWC} \bullet f(n) \tag{7}$$

where k is the constant of proportionality. We shall see that C_d and C_m can be obtained from k, which is easily obtained from simultaneous measurements of TAS, LWC, and $\mathrm{d}V/\mathrm{d}t$ in typical tunnel experiments. (Tunnels can usually be precalibrated in terms of LWC and TAS for a selected range of these variables.)

E. Relationship Between the Calibration Constants

The calibration constants C_m and C_d are related, as may be seen by combining Eqs. (2) and (3) to get

$$C_d = \mathrm{d}D/\mathrm{d}t/[C_m\,\mathrm{d}M/\mathrm{d}t] \tag{8}$$

This leads to some useful results. Substitution of Eqs. (5) and (6) into Eq. (8) gives

$$C_d C_m = \beta_{\max}/(E_{\text{tot}} \bullet \text{area} \bullet \rho) \tag{9}$$

The ratio of $\beta_{\max}$ to E_{tot} ranges only from 1.03 to 1.15 for all the pairs in Table 1, and so the product of C_d and C_m is practically constant within about $\pm 5\%$ at 0.0074 ± 0.0004 m/g.

By equating Eqs. (3) and (5) and substituting Eq. (7) for $\mathrm{d}V/\mathrm{d}t$, it is seen that k is related to C_d by

$$C_d k = \beta_{\max}/[\rho \bullet f(n)] \tag{10}$$

Similarly, equating Eqs. (2) and (6) and substituting Eq. (7) for $\mathrm{d}V/\mathrm{d}t$ shows that k is related to C_m by

$$k/C_m = E_{\text{tot}} \bullet \text{area} \tag{11}$$

Because k can be determined experimentally through Eq. (7), then C_d and C_m can be computed from Eqs. (10) and (11), if $\beta_{\max}$ and E_{tot} are known (and assuming that $f(n) = 1$).

Although values of k, C_d, and C_m generally differ from probe to probe, depending on the sensitivity and gain of the electronics with each individual probe, we see from Eqs. (9–11) and Table 1 that the products $C_d \bullet C_m$ and $k \bullet C_d$ and the quotient k/C_m should always be approximately the same constant values for all 0871FAs. For values of $\beta_{\max} = 0.95$ and $E_{\text{tot}} = 0.91$ (from Table 1 for 20-μm droplets at 200 kt) one gets from Eqs. (10) and (11)

$$k \bullet C_d = 1.04 \times 10^{-6}\ \text{m}^3 \cdot \text{g}^{-1} \quad \text{and} \quad k/C_m = 1.45 \times 10^{-4}\ \text{m}^2 \tag{12}$$

Equations (12) may be employed as probe-independent, universal calibration equations for obtaining C_d and C_m from k, which is

Table 1 Droplet collection efficiencies (from LEWICE) on a 6.35-mm-diam cylinder

		Droplet diameter								
		10 μm			15 μm			20 μm		
Altitude, km	TAS, kt	$\beta_{\max}$	E_{tot}	Ratio $\beta_{\max}/E_{\text{tot}}$	$\beta_{\max}$	E_{tot}	Ratio $\beta_{\max}/E_{\text{tot}}$	$\beta_{\max}$	E_{tot}	Ratio $\beta_{\max}/E_{\text{tot}}$
0	200	0.87	0.77	1.13	—	—	—	0.95	0.91	1.04
3	100	0.82	0.71	1.15	0.88	0.82	1.07	0.93	0.88	1.06
3	150	0.86	0.76	1.13	0.92	0.86	1.07	0.95	0.90	1.06
3	200	0.88	0.79	1.11	0.92	0.86	1.07	0.95	0.91	1.04
3	250	—	—	—	0.93	0.88	1.06	0.954	0.915	1.04
3	300	0.90	0.82	1.10	0.94	0.90	1.04	0.96	0.93	1.03
6	200	0.89	0.81	1.10	—	—	—	0.96	0.93	1.03

easily obtained from Eq. (7). Equations (12) are applicable to any 0871FA, and they are sufficiently accurate for most purposes. The user can fine-tune Eqs. (10–12) by selecting other combinations of β_{max} and E_{tot} from Table 1, if a more exact match to experimental conditions is desired.

III. Calibration Procedure

Two model 0871FAs, serial numbers 118 and 807, were taken to the Goodrich factory in Burnsville, Minnesota, for checkout and calibration in the factory icing wind tunnel. The following information focuses on the results obtained with 0871FA number 807, because it exhibited most of the interesting features.

A. Bench Tests

Before the calibration runs in the tunnel, the probes went through a standard factory bench test to document the initial condition of the probes. In addition to verifying the acceptable operation of the probes, including the proper functioning of the de-icing heater, the tests recorded the existing upper and lower limits of the analog output voltage. This range controls how much ice can accrete during each cycle until the heater is activated. The bench tests do not include any calibrations of the probe response to ice accretions.

The upper limit, V_{trip}, is the value of the analog output at which the heater is tripped, or activated. The factory-acceptable range for V_{trip} is 5 ± 0.5 V. The observed value of V_{trip} for probe 807 in its arrival condition was 4.85 V and was within the acceptable range.

The lower limit, V_0, is the value of the analog output voltage for the clean, uniced sensing tube. The factory-acceptable range for V_0 is 1 ± 0.7 V. The observed value of V_0 for probe 807 in its arrival condition was 2.2 V. This value is larger than the factory-acceptable range, but the only effect is to reduce the span $\Delta V = V_{trip} - V_0$ and, therefore, the amount of ice that can accrete before the heater is activated.

B. Calibrations in the Icing Wind Tunnel

The probes were calibrated in controlled, steady-state conditions of temperature, TAS, LWC, and droplet median-volume diameter (MVD) in the tunnel. The tunnel settings for the probe 807 tests are listed in Table 2. The intent was to select several airspeeds spanning the typical operating range for icing wind tunnels while keeping the LWC constant at a modest value. The static air temperatures (SAT) in the tunnel were kept sufficiently low to avoid Ludlam-limit effects [5] and the possible blowoff of water that may not immediately freeze upon impact. The MVD was nominally 20 μm for each run. Table 1 and later results show that for airplane speeds, the probes are practically insensitive to changes in MVD above 15 μm.

Probe 807 was operated first in its arrival condition (runs 1–4 with $V_0 = 2.2$ V) and then again after adjusting V_0 to 1.2 V (runs 9–11).

Table 2 Test conditions for probe 807 in the Goodrich tunnel (for LWC = 0.3 g/m^3 and MVD = 20 μm)

Run	TAS, kt	SAT, °C
1	280	−27
2	220	−24
3	220	−7
4	220	−7 to −16
9	120	−9
10	220	−9
11	280	−13

The only outputs of interest from the 0871FA for present purposes are the analog signal voltage rise rate dV/dt, the voltage span, and the cycle rise time. Under steady-state spray conditions, the output of the 0871FA should be a sawtooth voltage like that shown in Fig. 2. The value of dV/dt can be easily determined from the ascending ramp, and Δt is simply the time required for the analog output voltage to increase from V_0 to V_{trip}. The value of k can be computed from Eq. (7) for one or more runs, and then the constants C_d and C_m can be obtained from Eqs. (12).

Table 3 shows all the calibration information that can be obtained from a single run. The accuracy of the calibration depends on how well the variables in Eq. (7) are known and on having the temperature low enough to ensure 100% freezing ($n = 1$). In practice, the determining factors will be the uncertainty in the LWC used for the calibration and the scatter or irreproducibility in the corresponding dV/dt. A typical uncertainty of $\pm 10\%$ in each will result in the same order ($\pm 20\%$) of uncertainty in the calibration constants and in the indicated icing rates or amounts.

C. Nominal 0871FA Probe Calibration

The advertising literature and the factory instruction manual describe the generic 0871FA as having the following nominal values: $V_0 = 1$ V, $V_{trip} = 5$ V, and ice depth per cycle = 5 mm. From these, one can derive nominal values of the calibration factors C_m, C_d, and k, which can be compared with actual probe calibrations. Thus, for the nominal detector with a sensitivity of 0.5 mm of ice over a 4 V output range (1–5 V), the ice accretion rate in mm/s is given by

$$dD/dt = \frac{0.5 \text{ mm}}{4 \text{ V}} \bullet \frac{\Delta V}{\Delta t} = 0.125 \frac{\Delta V}{\Delta t} \tag{13}$$

from which $C_d = 0.125$ mm/V or 1.25×10^{-4} m/V.

The mass calibration constant, C_m, can be computed from Eq. (9), and the value of k can be obtained from Eqs. (12). These are listed in Table 4, which compares the calibration of the test probes with this nominal calibration.

Table 3 Summary of the calibration data for 0871FA probe 807 from run 10

Indicated tunnel settings:	TAS, m/s	LWC, g/m^3	MVD, μm	SAT, °C
	113	0.3	20	−9
LEWICE-computed values:	β_{max}	$f(n)$	E_{tot}	
	0.95	1	0.91	
	Measured values:			
Signal voltage span, ΔV=	3.45 V	$=(V_{trip} - V_o) = 4.85$ V − 1.4 V = 3.45 V		
Cycle rise time, Δt=	24 s	=0.40 min		
Voltage rise rate, dV/dt=	0.14 V/s	$=\Delta V/\Delta T$		
	Computed calibration constants:			
k=	0.0041 V/s per (m/s · g/m^3)	from Eq. (7)		
C_m=	28 V/g	from Eq. (12)		
C_d=	2.54×10^{-4} m/V	from Eq. (12)		
	Computed icing rates (converted to practical units):			
Icing depth rate, dD/dt=	2.1 mm/min	from Eq. (3) or (5)		
Depth per cycle, ΔD=	0.88 mm	$C_d \bullet \Delta V$ or $(dD/dt) \bullet \Delta t$		
Water catch rate, dM/dt=	4.9 mg/s	from Eqs. (2) or (6)		
Ice mass per cycle, ΔM=	123 mg	$=\Delta V/C_m$ or $(dM/dt) \bullet \Delta T$		
Mass per volt=	35 mg/V	$=1/C_m$ or $\Delta M/\Delta V$		

D. Meaning of Differences in Probe Calibrations

Anyone who reduces and compares data from different 0871FAs knows that the effect of differences or changes in the probe calibrations on the probe response can be confusing. To help clarify the relationship for the interested reader, we digress here to compare the response of probe 807 after adjustment, for example, to the nominal probe.

Referring to Table 4:

1) According to C_m, probe 807 was about half as sensitive as the nominal probe; thus, probe 807 required about twice as much ice as the nominal probe to produce a volt of output.

2) According to k, the voltage rise rate (V/s) was about half the rate of the nominal probe; thus, probe 807 took about twice as long as the nominal probe for the output voltage to increase by the same amount. This also means that probe 807 would underestimate icing rates by a factor of two *if* the factory-nominal calibration were assumed to apply to this probe.

3) If the probe 807 output voltage span were the same as for the nominal probe (4.0 V), then probe 807 would accrete twice as much ice (1 mm or 140 mg) per cycle as the nominal probe. But because the probe 807 span (3.45 V) is about 14% smaller than for the nominal probe, the ice actually accreted per cycle (0.88 mm or 123 mg) will be about 14% less than twice that for the nominal probe.

Basically, the calibration constants and the output voltage span together determine how much ice will accrete per cycle. The calibration constants determine how fast the output voltage increases for a given TAS and LWC, and the voltage span determines how far the voltage can go. Together, they determine how long the probe can accrete ice before the heater energizes.

IV. Observations on Probe Performance During Tunnel Tests

The operation of the 0871FAs in the tunnel gave the opportunity to view, via close-up video through a window on the test section, the ice accretion and shedding cycles. The controlled conditions allowed a study of the repeatability and any irregularities of the probe response. The principal observations are the following.

A. Ice-Shedding Difficulties

Some probes have difficulty shedding all the ice during the heater interval at some combinations of airspeed and temperature. For probe 807, the ice did not shed cleanly for airspeeds of 113 to 144 m/s and SATs lower than about −9°C. At the lowest airspeed of 62 m/s, there was great difficulty in removing the accreted ice when the SAT was below −20°C. Runs 3 and 10 were the only runs in which the ice shed cleanly every cycle: the ice melted and was quickly blown away. Runs 3 and 10 exhibited nearly ideal behavior, except for the several volts of overshoot.

During operation, a conformal, semicylindrical ice cap or sheath forms visibly on the windward side of the sensing tube. When the shedding difficulties occurred, one could see that the ice sheath debonded when the heater was on, but the sheath did not readily melt away or blow off. After the heater shut off, the partially melted ice cap would reattach to the sensing tube and cause the heater to immediately turn on again. Many of these sequential heater cycles were often required before the ice was completely removed. The result was not only an erratic-looking output voltage, but much more dead time (heater-on time) than normal. Figure 4 is a good example of this. From 120 to 400 s, the probe gave usable ramps of the analog output voltage, some of which were followed by two or three extra heater cycles. After 400 s, however, the signal became unusable due to incessant heater cycles caused by an apparent inability to melt and dislodge the ice at a low temperature of −27°C.

It was observed that *any* notch in the analog output signal was due to a piece of ice that did not shed and, therefore, affected the probe vibration frequency after it reattached.

According to Goodrich engineers, the problem of incomplete melting of the ice under certain conditions is due to the orientation of the de-icing heater within the sensing tube on the older models. This placement apparently does not concentrate enough heat on the upstream side of the tube to allow for complete ice removal during one heater cycle when operating at low temperatures and/or high icing rates. The problem has been mitigated in newer model detectors by adjusting the orientation of the heater in the sensing tube.

Another contributing factor may be that probe 807 (after adjustment of V_0) accretes about 75% more ice than the nominal probe during the sensing interval. This extra mass of ice may be more than the heater can melt in one heater cycle at low temperatures.

The other probe (118) shed ice cleanly at all speeds (62 to 144 m/s) and temperatures (−7 to −13°C) that were tested, and the output signal was nearly ideal with no overshoot. This clean shedding ability may be due to the relatively thin (0.3 mm) ice accumulation that forms on this particular probe before heater activation.

A close-up video of probe 807 during several runs revealed some other interesting characteristics of the ice accumulation and shedding.

1. *Run 9 at* 62 m/s *and* −9°C

Melting starts on the sides of the probe and progresses forward, but overall, the ice is slow to melt. The ice accretions often appear to be irregular in shape, especially if they are building on previously unshed accretions. The heater appears to stay on for long periods of time: tens of seconds.

There is also considerable difficulty in shedding the *meltwater* at 62 m/s. There is noticeable and persistent runback, with drops collecting in the recirculation zone on the back side of the sensor tube and the supporting strut. Drops even collect and circulate on the back side of the probe tip, where they may possibly refreeze when the heater stops. Evidently, the heat available at the backside of the probe is insufficient to quickly evaporate the drops of meltwater that collect there.

2. *Run 10 at* 114 m/s *and* −9°C

There is consistently clean de-icing of probe 807 at this airspeed. The ice melts and is quickly blown away.

Table 4 Comparison of tested 0871FA calibrations to the nominal calibration

	Nominal calibration	Probe 807 before adjustment	Probe 807 after adjustment	Probe 118	Probe 125
C_m, V/g	57	32	28	59	23
C_d, m/V	1.25×10^{-4}	2.2×10^{-4}	2.54×10^{-4}	1.2×10^{-4}	3.15×10^{-4}
k, V/s per (m/s · g/m^3)	0.0083	0.0047	0.0041	0.0085	0.0033
$V_{\text{trip}} - V_0 = \Delta V$	5 V − 1 V = 4 V	4.85 V − 2.2 V =2.65 V	4.85 V − 1.4 V =3.45 V	4.5 V − 1.5 V =3.0 V	4.2 V − 1.7 V =2.5 V
Mass (mg) per cycle = $\Delta V/Cm$	70	83	123	51	109
Mass (mg) per volt = $1/C_m$	17.5	31	35	16.9	43.5
Depth (mm) per cycle = $C_d \bullet \Delta V$	0.50	0.58	0.88	0.36	0.79
$k \bullet C_d$	1.04×10^{-6}	1.03×10^{-6}	1.04×10^{-6}	1.04×10^{-6}	1.04×10^{-6}
k/C_m	1.46×10^{-4}	1.47×10^{-4}	1.46×10^{-4}	1.44×10^{-4}	1.43×10^{-4}
$C_d \bullet C_m$	0.0071	0.0070	0.0071	0.0072	0.0072

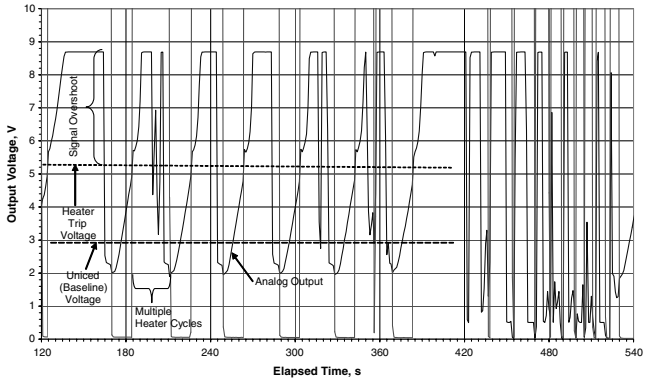

Fig. 4 Icing wind tunnel run 1 for 0871FA probe 807 (TAS = 280 kt, SAT = −27°C, and LWC = 0.3 g/m^3).

3. Run 11 at 144 m/s *and* −13°C

The probe sheds cleanly until about $12\frac{1}{2}$ min into the run when it unexplainably starts to accumulate unusually large ice buildups that are difficult to shed. Sometimes a piece of unshed ice remains clinging to the base of the sensing tube and contributes to the next cycle of buildup.

Conclusions from the video:

1) Low airspeeds (circa 62 m/s or less) may be insufficient to remove drops of runback meltwater from the probe. Refreezing of unshed drops may contribute to premature cycling of the heater.

2) At low SATs (sometimes as high as −7°C), the ice may not all melt during a single heater cycle. The ice rebonds and causes the heater to energize again and again until the ice is finally removed.

3) Probes that collect considerably more than the nominal 0.5 mm of ice may have more difficulty melting and shedding the accreted ice during a single heater activation, especially at low speeds and low air temperatures.

B. Signal Overshoot

Figure 2 illustrates the expected behavior of the signal output voltage, where it rises to the heater trip point V_{trip} (about 5.5 V in this figure) and then rapidly decreases to the baseline or below while the heater is on. In some probes, however, the analog output voltage regularly overshoots the heater trip voltage. Figure 4 shows the output voltage pegged at nearly 9 V for sometimes tens of seconds at a time. The reason for this overshoot in probe 807 is unknown. It is mainly a nuisance unless it lasts longer than a couple of seconds, in which case it increases the dead time of the probe by delaying the return to the sensing mode. This will give erroneous results if the user is counting cycles as a measure of LWC or icing intensity.

C. Ice Signal Duration

Each time the heater is energized, the 0871FA also outputs a 26 V ice signal, which lasts for about 5 s in this particular 0871FA. It is recorded in Fig. 4 as a series of thinly drawn square waves. This voltage is used for triggering a lamp or other warning device in the cabin of the airplane.

The tunnel tests reveal that, as a result of the heater retriggering, the ice signal often remains on for sometimes much longer than 5 s when the heater is having trouble removing the ice.

D. Shift in the Baseline Voltage

The bench tests included a measurement of the baseline analog voltage when the sensing tube is clean (uniced). The tunnel test results indicate that, during operation, the apparent V_0 can be a few tenths of a volt higher than that obtained from the bench tests. This occurred in some runs (not shown) where V_0 was about 2.5 V compared with the bench test value of 2.2 V. The operational value of V_0 can be difficult to determine when the output signal is erratic due to multiple heater cycles.

This shift in V_0 just means that the operational voltage span ΔV is a little less than the bench test value, and, therefore, the actual ice per cycle will be proportionately less than that implied by the bench test results.

E. Behavior as Surface Temperature Approaches 0°C

There is some practical interest in the performance of the ice detector when combinations of SAT and dynamic heating result in a surface temperature close to 0°C. Dynamic heating is proportional to the square of the airspeed and consists of compressional heating, which is concentrated along the leading edge, and frictional heating, which is distributed all along the forward-facing surface. There is also a contribution from the kinetic energy of the impacting droplets and the release of their latent heat of fusion upon freezing at the surface of the tube. Airspeeds of 100 to 300 kt will raise the surface temperature by 2° to 10°C, respectively. Ice accretion codes such as LEWICE take this into account, and Fig. 5 illustrates the effect for a 6.35-mm cylinder.

One may anticipate that as the surface temperature rises to 0°C, the icing rate would get slower until eventually no ice forms at all. That is, the slowing icing rate would be expected to reveal itself in the form of elongated accumulation intervals: that is, a flattening of the slope k, in Eq. (7). To observe this effect, one run with probe 118 was conducted with the tunnel air temperature slowly warming up. Figure 6 shows the results. The icing slowed due to a combination of increasing recovery time at the end of the heating intervals and a gradual decrease in slope k of $\mathrm{d}V/\mathrm{d}t$. The increasing recovery time is manifested as a gradually widening "shoulder" below the baseline. Tests seem to indicate that, all else being the same, the shoulder takes less time to complete, the greater the LWC.

In the top panel of Fig. 6, when the indicated total air temperature (TAT) was still −2 to −3°C, about 6 s was required for the signal to return to the baseline V_0 after the analog signal hit bottom. About 8 s was required for Δt, the signal rise time from $V_0 = 1.4$ V to $V_{\text{trip}} = 4.4$ V. About four icing cycles occurred each minute.

As the TAT continued to rise through 0°C (center panel), both Δt and the recovery time continued to increase by 1 or 2 s, but the icing did not stop. By the end of the center panel, the icing cycles had slowed to three per minute.

Finally, as the TAT rose above 1°C (lower panel), the slowing of the ice accretion was due mainly to increasingly longer delays between cycles. The rise rate $\mathrm{d}V/\mathrm{d}t$ was slowing too, and by TAT = 2°C it had decreased by 50%: Δt was now 12 s instead of 6 s. When the TAT reached about 2.5°C (36.5°F), no more ice accumulated at all.

The main impression was that, as the recovery time became very long (such as after the 930-s mark in Fig. 6), the onset of the next accumulation interval became unpredictable. When (or if) the accumulation decided to begin again, it did so suddenly and with a rate that seemed (to the eye) nearly as rapid as before. This intermittent behavior was also observed by Cober et al. [3], who recommended additional research on the phenomenon.

This is only a phenomenological study. Interpreted simply in terms of Fig. 5, the leading edge of the tube warms above freezing first, whereas the rest of the cylinder surface remains below 0°C, where ice can continue to form. As the SAT and TAT (and the curves in Fig. 5) continue to rise, the 0°C line moves back on the cylinder, reducing the area on which ice can form. Ludlam-limit effects (blowoff of water) retard the rate of ice accretion. The important factor is not the TAT, however, but the surface temperature that depends on the LWC as well as the TAT. A recent paper by Cook [6] gives a more detailed theoretical study of maximum air temperatures at which icing is expected to occur, depending on the Mach number and on the ambient relative humidity. Mazin et al. [7] also treat some of these subtleties.

F. Repeatability of the 0871FA Response

In a separate set of experiments, another probe (serial 125) was operated in the large icing research tunnel (IRT) at the NASA Glenn Research Center near Cleveland, Ohio. Figure 7 shows this 0871FA and several other probes mounted in the tunnel. Thirty-seven runs were conducted over a wide range of LWCs and drop size

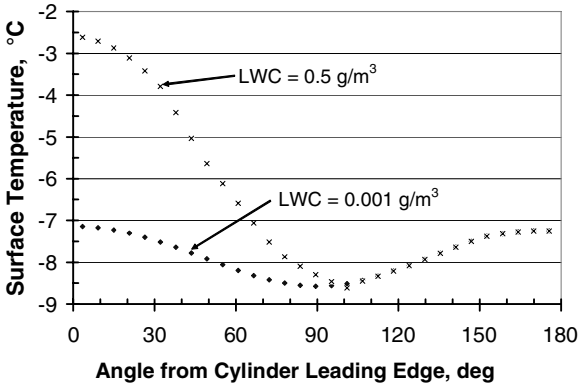

Fig. 5 LEWICE-computed surface temperature around the circumference of a 6.35-mm-diam cylinder with TAS = 150 kt at 3-km altitude and SAT = −10°C. The upper curve shows the increase due to the kinetic energy and latent heat of fusion of 15-μm droplets striking and freezing on the surface.

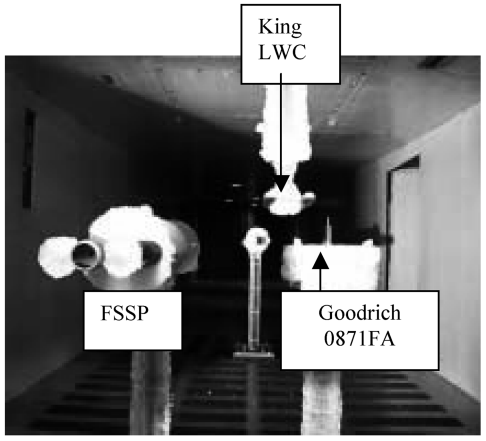

Fig. 7 The 0871FA, a King LWC probe, and an FSSP droplet size spectrometer in the NASA IRT. The 0871FA is clearly ice-free, except for the stand upon which it is mounted.

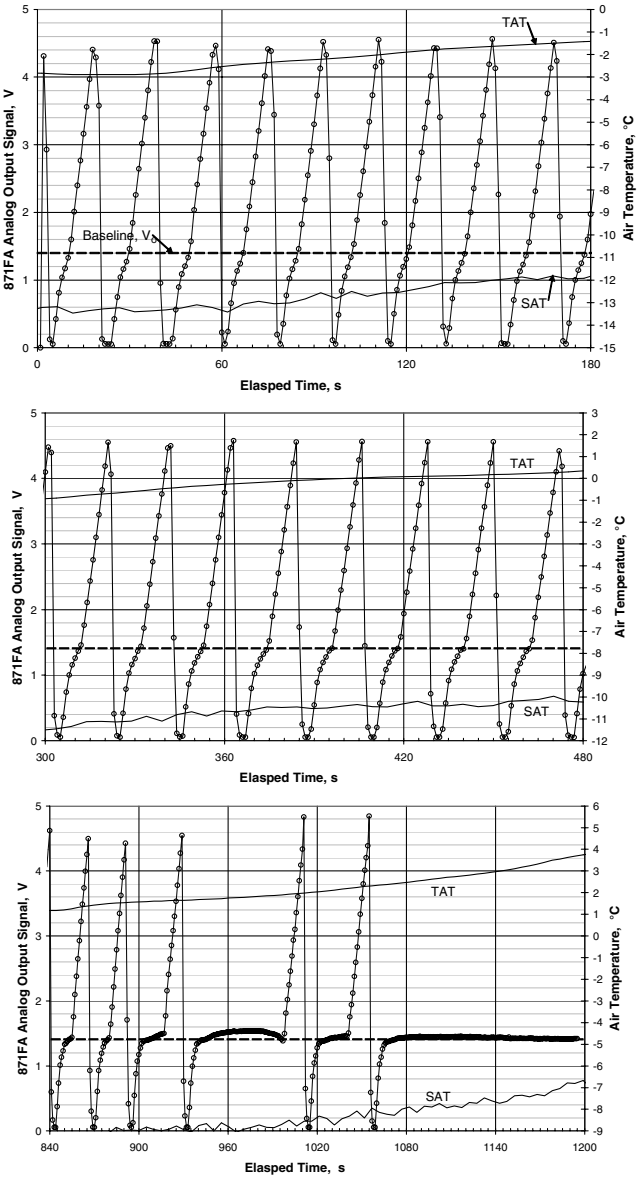

Fig. 6 Behavior of 0871FA (probe 118) output signal as temperature increases (for TAS = 280 kt and LWC = 0.3 g/m^3). The data points are 1 s apart. Be aware of the changing temperature and time scales between panels.

distributions at a constant air temperature (SAT) of −12°C and a constant airspeed of 67 m/s. Only the seven runs with LWCs less than 0.3 g/m^3 resulted in clean, nearly ideal voltage output ramps, as illustrated in Fig. 8. In all the other runs, the dV/dt signal was intermittently or continuously troubled by multiple heater cycles, the worst resembling that in Fig. 4. Two notable and unexplained exceptions were runs 5 and 37, both of which exhibited continually clean signals even though both had LWCs of 0.85 g/m^3 (and MVDs of 270 μm). The noisier the signal, due to multiple heater cycles, the more difficult it is to find useful ramps from which to compute a consistent slope and, therefore, the icing rate.

Figure 8 also shows fine-scale LWC variations as indicated by the so-called King probe [8]. In the NASA IRT, for LWCs of the order of 0.2 g/m^3 or less, momentary fluctuations appear to be as much as ±50%.

The last ten runs of the series were intended repeats of some of the earlier runs. Table 5 lists the pairs of repeat runs and the average icing rate indicated by probe 125 for each run. The right-most column shows that the 0871FA is repeatable, on average, despite some scatter from cycle to cycle, especially during the runs with irregular signals.

G. Uniform Response to Large Droplets

Figure 9 shows the results of 14 runs where the MVD ranged from 15 to 270 μm but the tunnel LWC was nearly constant at about 0.83 g/m^3. Ignoring one outlier[§] at 120 μm, there is no apparent trend in probe response with MVD over this range.

H. Linearity with LWC

Figure 10 shows the run average dV/dt as a function of the tunnel LWC setting for all 37 runs, regardless of MVD. Except for a small amount of scatter, the dV/dt is approximately linear with LWC up to 0.85 g/m^3 at least, for this temperature, airpeed, and MVD range.

I. Calibration of Probe 125

The previous calibration example (Table 3) showed how to obtain a calibration from a single test run. Figure 10 illustrates the fact that there is usually some scatter from run to run, even in controlled tunnel conditions, and so it may be preferable to base the calibration on the average response over a selected LWC range or over all the available runs.

Ideally, the data points should fall along a straight line, the slope of which can be used to calibrate the probe. Figure 10 includes a linear trendline (generated automatically by the spreadsheet software used

[§]This outlier, which also shows up as the upper data point above 0.8 g/m^3 in Fig. 10, has been noticed by other researchers [9] using the NASA IRT. It seems to be a miscalibration (underestimate) of the tunnel LWC for that setting.

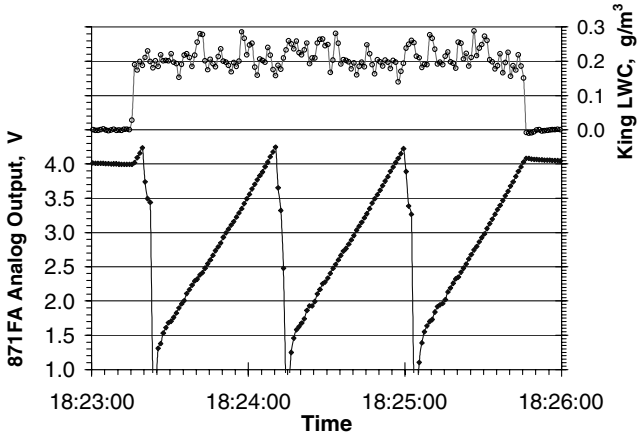

Fig. 8 Test run 9 for 0871FA probe 125 in the NASA IRT.

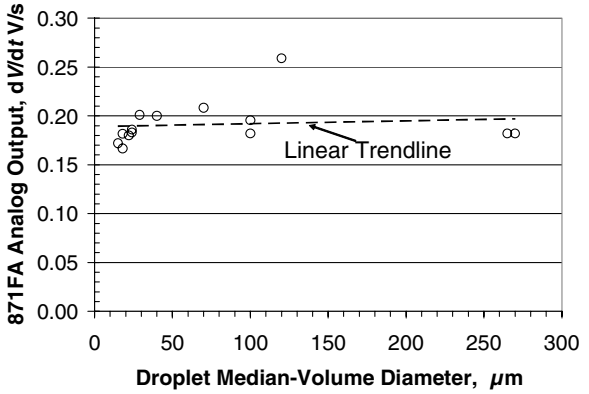

Fig. 9 Response of 0871FA probe 125 to drop size (MVD) for constant LWC (LWC = 0.83 ± 0.06 g/m³, TAS = 130 kt, and SAT = −10°C).

to produce this graph) to represent a best-fit average through the data points. The slope is 0.224 V/s per g/m^3. From Eq. (7), the slope in this case is equal to the product $k \bullet \mathrm{TAS}$ from which $k = 0.224/(67\ \mathrm{m/s}) = 0.0033$. Then, the other two calibration constants can be obtained from Eqs. (12), which gives

$$C_d = (1.04 \times 10^{-6})/k = 3.15 \times 10^{-4}\ \mathrm{m/V} \quad \text{and}$$

$$C_m = k/1.45 \times 10^{-4} = 23\ \mathrm{V/g}$$

These and other values are listed in Table 4. The accuracy of this calibration may be a little better compared with a single-point calibration, as in Table 3, because an average of several LWC measurements is used instead of relying on a single point. It depends, however, on how the analyst draws the line through the data. Instead of the single trendline used in Fig. 10, one could fit the data below 0.5 g/m^3 with one line and those above with another of different slope. For LWCs below 0.5 g/m^3, the scatter in $\mathrm{d}V/\mathrm{d}t$ appears to be about ±20% (which includes any uncertainty in LWC and any irreproducibility in $\mathrm{d}V/\mathrm{d}t$). As before, this ±20% would propagate through to the indicated icing rates and amounts.

V. Summary and Conclusions

1) A simple, new calibration scheme has been introduced that allows a complete calibration of model 0871FA icing detectors for ice mass-and-depth accretion rates and LWC from just the measured $\mathrm{d}V/\mathrm{d}t$ when TAS and LWC are known.

2) Older model 0871FAs may show anomalous irregularities in the analog output voltage signal if the ambient temperature is too low, the airspeed is too low, or the LWC too high. Close-up video demonstrated that this is due to incomplete shedding of ice during the heater cycle. The probes tested in this exercise exhibit clean output signals without interference from faulty de-icing when the LWC is less than about 0.3 g/m^3 and the air temperature is above about −7°C. For conditions outside these limits, more than one heater cycle may be needed to remove the accumulated ice before normal icing rate indication can resume.

Table 5 Repeatability of IRT tunnel settings and 0871FA icing rate

Run	Tunnel LWC, g/m^3	MVD, μm	Indicated icing rate, mm/min	Average icing rate,[a] mm/min
7	0.20	15	0.49 – 0.54	0.5
28	0.18	15	0.58 – 0.62	0.6
9	0.25	14	0.88 – 0.94	0.9
29	0.24	14	0.90 – 1.01	1.0
12	0.43	33	1.33 – 1.55	1.5
30	0.38	33	1.33 – 1.55	1.5
14	0.48	36	1.87 – 2.24	2.1
31	0.49	36	1.87 – 2.06	2.0
17	0.30	18	1.23 – 1.27	1.3
32	0.31	18	1.18 – 1.36	1.3
19	0.33	24	1.27 – 1.87	1.6
33	0.32	24	1.18 – 1.40	1.3
5	0.84	270	2.34 – 3.18	2.7
37	0.86	270	2.34 – 3.12	2.5

[a]Average icing rates rounded to one decimal place.

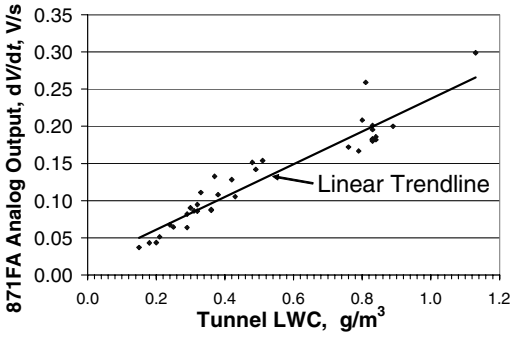

Fig. 10 Response of 0871FA probe 125 to LWC, regardless of drop size (MVD = 13 to 270 μm, TAS = 130 kt, and SAT = −10°C).

3) Operated in the *same* icing conditions, different 0871FAs can have output voltage rise rates that differ by up to a factor of 5 and ice accumulations per cycle that can differ by a factor of 2.5.

4) The response of the 0871FA is practically independent of the MVD over the tested range of 15 to 270 μm.

5) The indicated icing rate varies approximately linearly with LWC over the tested range of 0.15 to 0.85 g/m^3 (at −10°C and 67 m/s).

6) Although 0871FA icing detectors are often used on icing research flights, they seem to be overlooked as a useful tool in icing wind tunnels. As suggested in the Appendix, the combination of an 0871FA icing detector and a King LWC probe offers a convenient, portable set of probes for a) real-time checking and monitoring of spray settings in icing wind tunnels and b) *quantitatively* documenting the quality and reproducibility of sprays, such as for intercomparison of icing wind tunnels.

Appendix A: Uses of the 0871FA as a Regular Instrument in Icing Wind Tunnels

Icing rate meters seem to be an overlooked tool for icing wind tunnels, even though they are a natural choice. This Appendix points out two applications where an icing rate indicator ought to improve tunnel operations. Despite their ice-shedding difficulties, the older model 0871FAs can still be useful as long as the essential voltage output ramps ($\mathrm{d}V/\mathrm{d}t$) can be extracted. Newer model 0871FAs may be even better, as they promise fewer problems.

A. Checking, Monitoring, and Adjusting Spray Settings in Icing Wind Tunnels

It seems to be customary for operators of icing wind tunnels to check their LWC settings manually by measuring the depth of a small amount of ice collected on a thin blade or weighing the ice collected on a small cylinder or a set of rotating multicylinders from a timed exposure during a run [10,11]. The same checks can be done quickly, conveniently, and probably more accurately with an electronic probe like the 0871FA. Instead of manually weighing or measuring ice deposits, an automatic and real-time recorded readout like that shown in Fig. 8 seems much more useful and informative. The 0871FA permits the tunnel conditions to be monitored *continuously* in terms of dV/dt, icing rate, or LWC, as appropriate. A calibrated 0871FA can indicate the mass and depth of the deposited ice just like the blade or other cylindrical probes, but the 0871FA does it automatically and provides a continuous and permanent record.

The 0871FA would also indicate the onset of droplet freeze-out upstream of the test section if the wind tunnel temperature was set too low. The indicated ice accretion rate would decrease in proportion to the mass of the droplets turning to ice before reaching the icing detector. As described in Sec. IV, the 0871FA will also indicate the onset of incomplete freezing (Ludlam limit) if the tunnel temperature, airspeed, or LWC are set too high.

The inclusion of a LWC meter (as in Fig. 8) provides additional information. Not only can it continue to give an LWC reading when Ludlam-limit effects or reduced freezing fractions cause the ice accretion rate to slow on the 0871FA (or on any other accretion-based probe), but a fast-response LWC sensor can reveal the temporal uniformity (or departure therefrom) of the spray cloud. In Fig. 8, for example, the King LWC trace indicates that the LWC fluctuated continuously by as much as $\pm 33\%$ from the mean LWC value of 0.21 g/m^3. This fluctuation was not due to detector noise, because when the spray was off (the airspeed still up), the LWC signal settled to a quiet and flat reading of zero, as seen at either end of the upper trace in Fig. 8.

A real-time readout would enable the tunnel operators to respond immediately to any offset from the desired tunnel settings and to fine-tune the settings as necessary. As it is now, operators set the water and air pressures in the spray nozzles to predetermined values as best they can. This sometimes results in LWCs that differ by $\pm 10\%$ or more from the desired value, but the amount of deviation is not known until an accretion probe is inserted into the tunnel and retrieved for manual weighing or measuring. Usually, rather than adjusting the settings to get closer to the desired LWC, it is simpler for the operators to keep the tunnel at that condition and just make a note of the actual LWC for reference. With a real-time readout, however, the TAS could be adjusted within reasonable limits to fine-tune the icing rate to a more precise value. The slope of the dV/dt ramp in Fig. 8 would seem to be a better discriminator for this fine-tuning than a noisy-looking LWC signal.

B. Use of an 0871FA Ice Detector for Intercomparison of Icing Wind Tunnels

Recently, there was a collaborative exercise [11] among a number of tunnel operators in Europe and North America to find out if all the tunnels would produce the same ice shape on a standard test article for the same tunnel settings. The resulting ice shapes differed by varying amounts from one another, but it was not known whether the differences were due to differences in the spray clouds or to uncertainties in the calibration of the individual tunnels. Some tunnels were calibrated using the manual accretion methods mentioned previously, and some used hot-wire LWC meters and modern electro-optical droplet size spectrometers. In either case, there were problems that left the reliability of the tunnel calibrations uncertain. With each tunnel crew using its own calibration methods and equipment, there was no way to exactly compare the spray conditions for each tunnel.

If an 0871FA and King LWC probe were circulated among the participating tunnels, a simple electronic record like that in Fig. 8 would be preserved and available for reference for each tunnel. The top trace would reveal the relative LWC and uniformity of the spray clouds (even if the exact calibration of the LWC probe were unknown). The lower trace would allow the tunnels to be compared in terms of dV/dt or *icing rate*: a meaningful variable not previously used for this purpose.

Presently, international efforts to intercompare tunnel sprays depend on comparing ice accretion shapes on a common test article circulated among the tunnels. This is a rather qualitative method using only time-integrated ice shapes that are sometimes difficult to measure and compare. The King LWC and 0871FA could improve the tunnel comparisons by providing directly intercomparable, quantitative engineering data (icing rate and fine-scale variability of LWC) on a second-by-second basis. These are two quantitative measurements that are easy to interpret and would complement current reliance on ice shape comparisons for tunnel comparisons.

For these tunnel intercomparisons, instead of setting up to a presumed and possibly uncertain LWC, the tunnel operators could all tune to the same icing rate (or dV/dt) as indicated by a reference 0871FA sent to each tunnel for use during the comparison runs. Any fine-tuning of dV/dt could be done by varying the tunnel airspeed rather than the possibly coarser adjustment of water and air pressures. As before, the real-time electronic readout avoids the delays and errors of spot accretion measurements and makes faster fine-tunings possible. It also leaves a permanent record of the spray condition for documentation and possible later analyses and comparison.

These two probes also have the advantage of being small so that they can fit in most tunnels. (Of course, in smaller tunnels, there may be some blockage problems unless the bulkier parts of the probes can be kept outside of the tunnel wall, or unless the supporting strut on the 0871FA can be elongated, or unless the probes can be operated upstream or downstream of the constricted test section.) Also, 0871FAs with little or no ice-shedding problems would have to be selected for use at low temperatures and/or high LWCs.

Acknowledgments

The help of the icing engineering staff (James Liao, John Severson, and Darren Jackson) at the Goodrich icing wind tunnel is gratefully acknowledged. The author is indebted to Walter Strapp of the Canadian Meteorological Service and to Dean Miller and Ed Emery of the NASA Glenn Research Center for obtaining the data in the NASA IRT. Manny Rios of the FAA Technical Center performed the LEWICE runs. Suggestions by two anonymous reviewers are appreciated.

References

[1] Baumgardner, D., and Rodi, A., "Laboratory and Wind Tunnel Evaluations of the Rosemount Icing Detector," *Journal of Atmospheric and Oceanic Technology*, Vol. 6, No. 6, 1989, pp. 971–979.

[2] Claffey, K. J., Jones, K. F., and Ryerson, C. C., "Use and Calibration of Rosemount Ice Detectors for Meteorological Research," *Atmospheric Research*, Vol. 36, 1995, pp. 277–286.

[3] Cober, S. G., Isaac, G. A., and Korolev, A. V., "Assessing the Rosemount Icing Detector with In-situ Measurements," *Journal of Atmospheric and Oceanic Technology*, Vol. 18, No. 4, 2001, pp. 515–528.

[4] Wright, W. B., "User Manual for the NASA Glenn Ice Accretion Code LEWICE Version 2.0," NASA CR-1999-209409, 1999; also http://icebox.grc.nasa.gov/LEWICE [cited 26 June 2006].

[5] Ludlam, F. H., "The Heat Economy of a Rimed Cylinder," *Quarterly Journal of the Royal Meteorological Society*, Vol. 77, Oct. 1951, pp. 663–666.

[6] Cook, D. E., "Maximum Temperature for Ice Accumulation Calculations," AIAA Paper 2005-0655, Jan. 2005.

[7] Mazin, I. P., Korolev, A. V., Heymsfield, A., Isaac, G. A., and Cober, S. G., "Thermodynamics of Icing Cylinder for Measurements of Liquid Water Content in Supercooled Clouds," *Journal of Atmospheric and Oceanic Technology*, Vol. 18, No. 4, 2001, pp. 543–558.

[8] King, W. D., Parkin, D. A., and Handsworth, R. J., "A Hot-Wire Liquid Water Device Having Fully Calculable Response Characteristics," *Journal of Applied Meteorology*, Vol. 17, No. 12, 1978, pp. 1809–1813.

[9] Strapp, J. W., Oldenburg, J., Ide, R., Lilie, L., Bacic, S., Vukovic, Z.,

Oleskiw, M., Miller, D., Emery, E., and Leone, G., "Wind Tunnel Measurements of the Response of Hot-Wire Liquid Water Content Instruments to Large Droplets," *Journal of Atmospheric and Oceanic Technology*, Vol. 20, No. 6, 2003, pp. 791–806.

[10] Anon., "Calibration and Acceptance of Icing Wind Tunnels," Society of Automotive Engineers, Aerospace Recommended Practice ARP5905, Warrendale, PA, Sept. 2003.

[11] Anon., "Icing Wind Tunnel Interfacility Comparison Tests," Society of Automotive Engineers, Aerospace Information Report AIR5666, Warrendale, PA, 2006.